

# Multi-pulses dynamic patterns in a topological insulator mode-locked ytterbium-doped fiber laser

Yan Peiguang<sup>a</sup>, Lin Rongyong<sup>a</sup>, Zhang Han<sup>b</sup>, Wang Zhiteng<sup>b</sup>,  
Chen Han<sup>a</sup>, Ruan Shuangchen<sup>a,\*</sup>

<sup>a</sup> Shenzhen Key Laboratory of Laser Engineering, Shenzhen University, Shenzhen 518060, China

<sup>b</sup> Key Laboratory of Optoelectronic Devices and Systems of Ministry of Education and Guangdong Province, Shenzhen University, Shenzhen 518060, China

## ARTICLE INFO

### Article history:

Received 2 August 2014

Received in revised form

31 August 2014

Accepted 3 September 2014

Available online 18 September 2014

### Keywords:

Topological insulator

Mode-locked fiber laser

Multi-pulses

Quasi-square pulses

## ABSTRACT

Multi-pulse dynamic patterns have been experimentally observed in an Ytterbium-doped fiber laser passively mode locked by a topological insulator (TI)  $\text{Bi}_2\text{Te}_3$  saturable absorber (SA). The fundamental mode-locking operation with a repetition rate of  $\sim 1.10$  MHz was achieved under a pump power of  $\sim 160$  mW with an appropriate setting of the polarization controller (PC). It was found that through either changing the pump power or rotating the orientation of intra-cavity PC, several characteristic modes have been experimentally observed, including disordered multi-pulses, bunch of pulses, and soliton rains. Simultaneously, quasi-square pulses have also been observed in the laser cavity. Our systematic study clearly demonstrated that TI could be developed as an effective SA for the generation of different pulse operation states in a passively mode-locked all-normal-dispersion Ytterbium-doped fiber laser.

© 2014 Elsevier B.V. All rights reserved.

## 1. Introduction

Passively, mode-locked fiber lasers have attracted much attention as a useful tool for the investigation of multi-soliton nonlinear dynamic [1–4]. It has been shown that various mechanisms had been proposed to interpret the formation of multi-solitons in an anomalous dispersive cavity, including the soliton shaping of dispersive waves, the effective spectral filtering effect, the wave-breaking effect and the soliton peak clamping effect. Indeed, various modes of multi-soliton operation have been observed in previous experimental, including bound solitons [5,6], disordered bunched multi-soliton [7,8], soliton rains [9–11], high-order harmonic mode-locking (HML) [12,13].

In compare with the erbium-doped fiber lasers, it was more difficult to achieve the formation of multi-pulses in the ytterbium-doped fibers due to its relatively larger spectral gain bandwidth in [2], but multi-pulses could be still obtained if the pump power was higher than some value [14,15]. However, most of the previous experimental studies on the multi-soliton operation states were concentrated on fiber lasers passively mode-locked with nonlinear amplifying loop mirror (NALM) [16] and the nonlinear polarization rotation (NPR) technique [12]. The usage of real passive saturable absorber (SA) seemed to be more advantageous for the development of commercial

mode-locked sources because NPR and NALM mode-locked laser were environmentally more sensitive, and it would be important to investigate multi-soliton characteristics in fiber lasers passively mode-locked based on a SA, such as semiconductor saturable absorbers (SESAM) [17], single-walled carbon nanotube (SWNT) [18–21] and graphene [22–30]. However, SESAMs had a narrow broadband response (a few tens of nanometers) and required complex fabrication process including integration and packaging. Moreover, SWNTs always resulted in non-saturable loss, and restricted its applications due to its response spectral range that was determined by the diameter and chirality. Although graphene had the broadband response, it had a relatively low damage threshold and low saturation intensity, which may further limit the pulse energy.

Mostly recently, a new type of Dirac nanoscale material named “topological insulator (TI)” [31–36], which has been successfully demonstrated as an effective saturable absorber material for the passive Q-switched or mode-locking in fiber lasers or solid-state laser at different wavelengths [37–47]. Those experimental results demonstrated that TI-SA had a broadband response wavelength range of saturable absorption, large modulation depth, high damage threshold and strong saturation intensity. It was demonstrated that introducing proper high nonlinear effect into the laser cavity was favorable for generating multi-solitons [48], and TI was experimentally found to show very large nonlinear refractive index (a value of  $10^{-14}$  m<sup>2</sup>/W) [49]. This indicated that TI played an important role on the formation of multi-soliton in mode-locked fiber lasers. Chen et al. have experimentally studied the formation of various multi-soliton patterns in a

\* Corresponding author.

E-mail address: [scruan@szu.edu.cn](mailto:scruan@szu.edu.cn) (R. Shuangchen).

mode-locked Erbium-doped fiber laser based  $\text{Ti}:\text{Bi}_2\text{Te}_3$  SA [50]. However, no previous work reported the multi-pulse in a  $\text{Ti}:\text{Bi}_2\text{Te}_3$  based mode-locked ytterbium-doped fiber laser, and the corresponding formation behavior of multi-pulse in such lasers still needed to be explored.

In this paper, we reported on the generation of multi-pulse operation states from all-normal dispersion ytterbium-doped fiber ring laser passively mode-locked by  $\text{Ti}:\text{Bi}_2\text{Te}_3$  SA, which was sandwiched between two optical fiber connectors through the optical deposition approach [51–53]. The fundamental mode-locking operation was achieved under a pump power of  $\sim 160$  mW with an appropriate setting of the polarization controller (PC). By adjusting the pump power and the orientation of the PC, it has been found that multi-pulse operation exhibited several characteristic operations from disordered multi-pulse, bunch of pulses, and soliton rains. Besides the above mode-locking operation states, quasi-square pulses could be also observed in the cavity under appropriate pump power and orientation of the PC.

## 2. Sample preparation and experimental setup

The layered  $\text{Bi}_2\text{Te}_3$  nano-sheets were synthesized by the liquid exfoliation approach, which had been elaborated in Ref. [37], and the inter-band relaxation time of  $\text{Bi}_2\text{Te}_3$  was  $\sim 0.5$  ps [54]. The corresponding scanning electron microscope (SEM) image was shown in Fig. 1(a), it could be obviously seen that the TI nano-material had a quasi-two-dimensional structure with regular hexagonal shape. The X-ray diffraction (XRD) pattern of TI nanosheets (PDF Card: 15-0863) showed a high [0 0 6] orientation and some characteristic peaks [0 1 5 and 0 0 1 5], as shown in Fig. 1(b).

Then  $\text{Bi}_2\text{Te}_3$  nano-sheets were dissolved in distilled water and leading to an efficient dispersion through 3 h of ultra-sonication. The uniform dispersion of  $\text{Bi}_2\text{Te}_3$  nano-sheets was suitable for optical deposition. In the following, a continuous wave (CW) single mode laser diode (LD) with central wavelength of 975 nm and maximum power of 500 mW spliced with a standard fiber connector (FC–PC) was used as the laser source for optical deposition, then light exiting from the fiber connector end-facet could be directly injected into the dispersion solution. The corresponding experimental setup was shown in Fig. 2. After 2-min light illumination under a pump power of 60 mW,  $\text{Bi}_2\text{Te}_3$  nano-sheets could be gradually adsorbed and deposited onto the fiber connector end-facet due to optical trapping force and heat convection effects. After being dried in ambient environment for one day, the fibered topological insulator based optical device was fabricated after connecting with another clean and dry fiber connector. The inset of Fig. 2 showed that part of the fiber

connector end-facet, and it could be clearly seen that the fiber connector core area was fully covered by the TI sample.

The saturable absorption property of the  $\text{Ti}:\text{Bi}_2\text{Te}_3$  sandwiched between optical fiber connectors was shown in Fig. 3. The laser source used was home built mode-locked laser oscillator with a repetition rate of 5 MHz and 150 ps operating at  $\sim 1064$  nm. The data obtained from the experiment was then fitted according to

$$\alpha(I) = \alpha_0 \left( 1 + \frac{I}{I_{\text{sat}}} \right)^{-1} + \alpha_{\text{ns}} \quad (1)$$

where  $I$  was the input laser intensity,  $I_{\text{sat}}$  was the saturation intensity (the intensity with the absorption coefficient of half the initial value),  $\alpha(I)$  was the intensity-dependent absorption coefficient, and  $\alpha_0$  and  $\alpha_{\text{ns}}$  were the modulation depth and the non-saturable loss, respectively. The results gave a saturation intensity of  $\sim 24.6$  MW/cm<sup>2</sup>, modulation depth of  $\sim 16.2\%$ , and non-saturable loss of  $\sim 22.8\%$ .

Our fiber laser was schematically shown in Fig. 4. The laser was pumped by a 976 nm pump laser through a wavelength division multiplexer (WDM), and the output of the laser was coupled through a 10% fiber optical coupler (OC). A segment of  $\sim 3.4$  m YDF with absorption of 250 dB/m@975 nm was used as the gain medium. A polarization independent isolator (ISO) was used to ensure the unidirectional operation of the ring laser cavity, and a three-spool polarization controller (PC) was employed to adjust the cavity birefringence. A bandwidth filter with a central wavelength of 1064 nm and 3 dB bandwidth of  $\sim 5$  nm was inserted into the cavity. A total length of  $\sim 180$  m HI-1060 Flex single mode fiber (SMF) was also incorporated to the cavity. The total cavity length was  $\sim 185$  m. The monitoring of the output temporal pulse trains and optical spectrum were performed using a 20-GHz mixed signal oscilloscope (Tektronix MSO72004C) with a 45-GHz

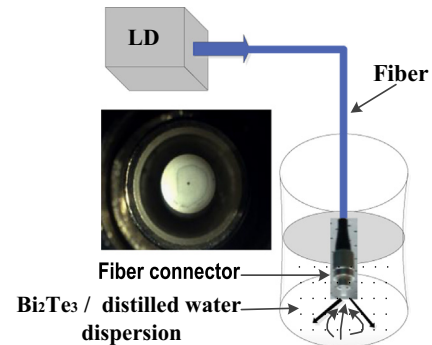


Fig. 2. Schematic diagram of optical deposition for  $\text{Ti}:\text{Bi}_2\text{Te}_3$ . Inset: Optical image of the fiber connector end-facet after deposition.

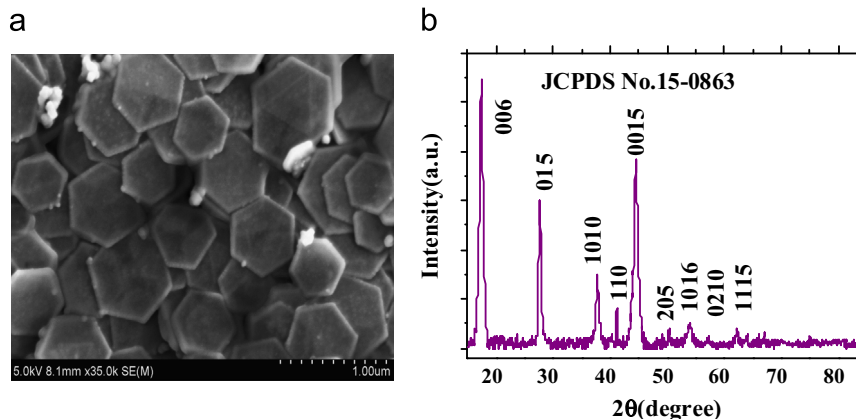


Fig. 1. (a) SEM image of the  $\text{Bi}_2\text{Te}_3$  nano-sheets. (b) The corresponding XRD diffraction pattern.

Download English Version:

<https://daneshyari.com/en/article/1534161>

Download Persian Version:

<https://daneshyari.com/article/1534161>

[Daneshyari.com](https://daneshyari.com)